Proceedings of the 28th Conference
on Decision and Control
Tampa, Florida • December 1989

Vibration Damping and Robust Control of the JPL/AFAL Experiment Using μ-Synthesis

Gary J. Balas
Aeronautical Engineering, 105-50
California Institute of Technology
Pasadena, CA 91125

Cheng-Chih Chu
Jet Propulsion Laboratory, MS 198-326
California Institute of Technology
Pasadena, CA 91109

John C. Doyle
Electrical Engineering, 116-81
California Institute of Technology
Pasadena, CA 91125

Abstract

The technology for controlling elastic deformations of flexible structures is one of the key considerations for future space initiatives. A vital area needed to achieve this objective is the development of a control design methodology applicable to flexible structures. In this paper, the μ-synthesis technique is employed to design a high performance vibration attenuation controller for the JPL/AFAL experimental flexible antenna structure. The results presented deal primarily with the control of first two global flexible modes using only two hub actuators and two hub sensors. Implementation of the multivariable control laws, designed based on a finite element model, are presented. All results are from actual implementation on the JPL/AFAL flexible structure testbed.

1 Introduction

The technology for controlling elastic deformations of large flexible structures is one of the key considerations for future space initiatives. A vital area needed to achieve this objective is the development of a control design methodology applicable to flexible structures. To that end, this research employs μ-based control design methods for the analysis and synthesis of controllers to lightly damped flexible structures. The JPL/AFAL flexible experimental antenna structure provides a testbed for validation of this control methodology and exploration of critical robust control issues.

The initial results deal primarily with design of a high performance vibration attenuation controller for the JPL/AFAL experiment using only the hub actuators and sensors to control the first two global flexible modes. The structural model used for the control designs is from the preliminary identification results documented in [1]. By pairing sensors and actuators properly, the model can be regarded as two decoupled single-input/single-output (SISO) systems which include two modes respectively. From experiments, little coupling of these two subsystems is observed.

Multi-Input/multi-output (MIMO) control laws are formulated using additional rib actuators/sensors. The goal is to improve the vibration attenuation using robust multivariable design techniques. A finite element model is used for control design since no identified model is available. The damping values are based on previous single-input/single-output experiments. The first boom-dish mode is assigned 12% critical damping, the second boom-dish mode 0.7% and all other modes 1% damping. The finite element model produces a number of modes between 0.09 and 4.5 Hz which are not included in the control design model. The neglected modes and the variations between the actual structure and the model are accounted for by the addition of uncertainty models.

The μ-framework allows for the incorporation of structured and unstructured uncertainty associated with the models into the controller design. The focus of the paper is on robust control for flexible structures with both unstructured and structured uncertainty due to unmodeled dynamics, actuator and sensor dynamics, and uncertainties in damping, frequencies and mode shapes. In the future, the abundance of actuators and sensors on the JPL/AFAL experiment will allow us to address a more challenging problem in large flexible structures, that is, robust control of flexible structures with numerous uncertainties using non-collocated sensors and actuators [2].

The control laws presented were designed using μ-synthesis techniques. Several different control designs were formulated in both the SISO and MIMO cases, however, only the designs which yielded the best closed-loop performance are discussed. All results are from actual implementation on the JPL/AFAL flexible structure testbed.

The paper is organized as follows. The JPL/AFAL experimental facility is described briefly in Section 2. Section 3 reviews the fundamental ideas of the μ-synthesis methodology. Problem formulation and controller synthesis procedure is presented in Section 4 and the analysis and experimental results are shown in Section 5.

Definitions

Terms to be used in this paper:

Nominal Stability (NS) The nominal plant model has to be stabilized by the controller design. This is a minimum requirement.

Nominal Performance (NP) In addition to stability, the quality of the nominal closed-loop response should satisfy some performance requirements. The performance is defined in terms of the weighted H_∞-norms for the closed-loop system between the exogenous inputs (disturbances) and "errors" (sensor outputs). This norm describes the worst cases closed-loop response, over frequency, to disturbances.

Robust Stability (RS) The closed-loop system must remain stable for all possible plants as defined by the uncertainty descriptions.

Robust Performance (RP) The closed-loop system must satisfy the performance requirement for all possible plants as defined by the uncertainty description. For example, a requirement may be

$$\overline{\sigma}(W_1(I+GK)^{-1}W_2) \leq 1 \ \ \forall\omega, \ \forall G$$

where W_1 and W_2 are frequency dependent weighting, G is a general interconnection structure, and $\overline{\sigma}$ is the maximum singular value.

2 Description of Experiment Facility

Experimental demonstration and verification of robust control using μ-synthesis techniques was conducted on the JPL/AFAL Flexible Structure Testbed. The testbed is a 3-D antenna-like structure which exhibits many characteristics of a typical large space structure. These include numerous low frequency modes, densely packed modes, low structural damping, and three-dimensional structural interaction among components. In this section, a brief description of the testbed facility is given. Detailed description can be found in [1,3].

2.1 Configuration

The main component of the testbed facility is shown in figure 1. It consists of a central rigid hub to which is attached 12 ribs The ribs are coupled by two rings of pretensioned wires. Functionally, the wires are intended to simulate the coupling effects of a reflective mesh installed over the rib frame in an actual antenna. The ribs are 2.25 m in length. The hub is of radius 0.6 m, making the dish structure 5.7 m in diameter. The tensioning wires make two rings at approximate diameters of 3 m and 4.8 m around the structure. Each

CH2642-7/89/0000-2689$1.00© 1989 IEEE

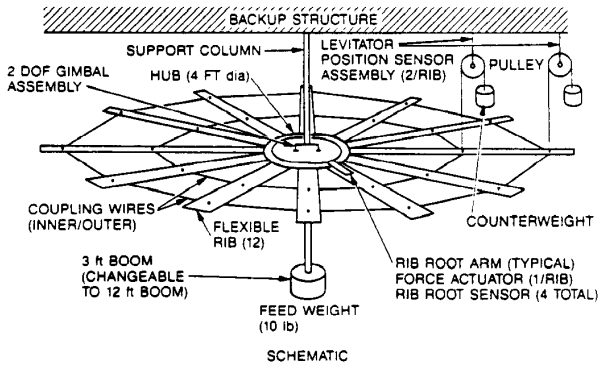

Figure 1: JPL/AFAL Flexible Structure Testbed

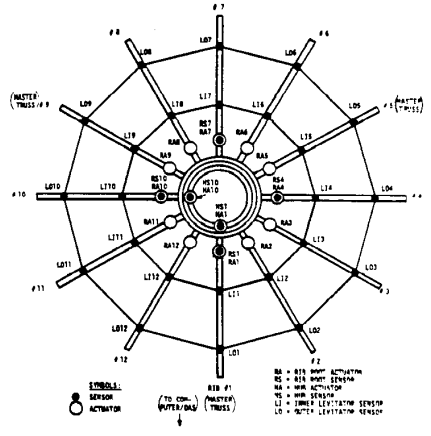

Figure 2: Assignment of Rib Number and Sensors/Actuators

rib is supported at its 40% and 80% points, 0.9 m and 1.8 m from the rib root, the same locations as the coupling wire attachments. A 1 m flexible boom is attached to the central axis of the hub and has a mass at its lower end to simulate the feed horn of an antenna. The feed mass is 4.5 kg. The hub is mounted to a backup structure via a two-axis gimbal which allows rotational freedom about two perpendicular axes in the horizontal plane. The gimbal bearings support approximately one quarter the weight of the ribs, the entire weight of the hub, boom, and feed, and their respective sensing and actuation devices.

2.2 Actuators

Each of the ribs can be excited dynamically by a single rib-root actuator, a lever arm of about 0.3 m from the hub attachment point. Each rib-root actuator consists of a speaker-coil type device which reacts against a mount rigidly attached to the hub. In addition to the rib-root actuators, two speaker coil type actuators are mounted on the hub to provide controlled torquing about the two gimbal axes. These hub torquers apply linear forces to the hub at its outer circumference to yield the required torques about the axis of rotation. Together, these 14 actuators are capable of controlling all flexible modes of the structure. The location of these actuators are shown in figure 2, together with the assignment of the rib numbers. As is, the axes of rotation are construed to be along rib#1 and rib#7, and rib#4 and rib#10, with respective rotations excited by hub actuators HA10 and HA1. For convenience, the axes are labeled as the 1-7 axis and 4-10 axis in all later references.

2.3 Sensors

Each of the 24 levitators is equipped with an incremental optical encoder which measures the relative angular rotation of the levitator pulley. These angular measurements are translated into the vertical motion of the ribs at the levitator/rib attachment points, relative to the backup structure. Additional linear variable differential transformers (LVDT) sensors are provided to determine the rib displacement measurements at four evenly spaced rib root actuator locations. Hub angular rotations about the two axes are measured by two rotary variable differential transformers (RVDT) mounted directly at the gimbal bearings. The locations of the 30 sensors are also shown in figure 2. As assigned, angular displacement about the 1-7 axis are measured by sensor HS1, and that about the 4-10 axis by sensor HS10.

The controller order and the number of control inputs and outputs are limited due to the constraints of the realtime computer. Only the hub and collocated rib sensors/actuators associated with the 4-10 axis in figure 2 are used in the multivariable designs (i.e. HA10/HS1, RA4/RS4, and RA10/RS10). The antenna is highly symmetric, therefore the 1-7 and 4-10 axis can be examined independently when using the finite element model.

2.4 Dynamic Model

The finite element method was used to generate a theoretical system model for the testbed structure. Simply, the method approximates the original distributed parameter system with its unlimited number of degrees of freedom by a discrete system with finite dimensionality. The symmetry of the dish structure makes it possible to separate variables and express a given mode shape as the product of a shape function, which is independent of the rib number, and a scalar function which depends on the rib number. This scalar function, which reflects the circular dependence of the given mode shape, can be written by inspection in the following form:

$$Sin\left[\frac{2\pi ik}{n} + \phi_k\right] \tag{2}$$

where i is the number of the rib, n is the number of ribs in the dish structure (12 in this case), and k is the circular wave number for a given mode ranging from $k = 0$ to $k = 6$, and ϕ_k is phase angle depending on the coordinate system transformation. A mode is completely specified by its frequency, circular wave number, phase angle, and the boom and rib shape functions.

2.5 Mode Shapes and Frequencies

Mode shapes of the structure can be grouped according to their circular wave number k. For $k = 0, 2, 3, 4, 5, 6$, all reaction forces on the hub caused by rib motion cancel out, and thus neither hub nor boom motion is involved in these modes. They behave as if the hub was clamped in its resting position and are called dish modes. As such, degrees of freedom of the hub and boom can be taken out, reducing further the dimension of the eigenvalue problem associated with the dish modes to 20. In addition, the dish modes corresponding to $k = 2, 3, 4, 5$ are each two-fold degenerate, while degeneracy does not exist for $k = 0$ and $k = 6$. This is due to the fact that for $k = 0$ and $k = 6$, modal excitations about the two orthogonal gimbal axes generate identical motion for the ribs and thus constitute as one mode. The frequencies of the first 20 dish modes are listed in Table 1.

For $k = 1$, the reaction forces on the hub do not cancel, and the modes appear as a rocking of the entire structure. These modes are called boom-dish modes as they involve motion of the boom, hub, and dish structure together. For a perfectly symmetric structure, the "boom-dish modes" are degenerate. However, for the present structure of which the hub is not quite symmetric, they are not. Table 2 show the modal frequencies of the first 12 boom-dish modes, 6 for each of the gimbal axes. The small differences in the frequency values reflect the slight hub non-symmetry.

It is noted that the dish modes, with their symmetric mode shapes about the hub, are not controllable and observable from the hub. Thus, hub actuation would manage only to excite and control the boom-dish modes. Since these modes constitute a small subset of all system modes, and larger frequency separation, they provide a good first test problem for initial experiment using μ-based controller. The SISO robust control experiments described investigate only the boom-dish modes via actuation/measurement at the hub. Work involving control of both boom-dish and dish modes is discussed in the multivariable control design section.

3 Robust Control Methodology

This section briefly reviews the frequency-domain methods for analyzing the performance and robustness properties of feedback systems using μ [3-7]. The general framework used in the paper is shown in figure 3. Any linear interconnection of inputs, outputs and commands along with perturbations and a controller can be viewed in this context and can be rearranged to match this diagram.

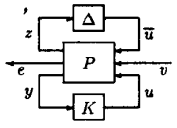

Figure 3: General Interconnection Structure

Figure 4: (a) Analysis and (b) Synthesis Problem

3.1 Analysis Overview

For the purpose of analysis, the controller may be thought of as just another system component. The inclusion of the controller into the plant reduces the diagram in figure 3 to that in figure 4-(a). The analysis problem involves determining whether the error e remains in a desired set for sets of input v and perturbation Δ. The uncertainty in v and Δ as well as the performance specifications on e are normalized to 1. This requires that all weighting functions and scalings be absorbed into the interconnection structure G. Furthermore, G can be partitioned so that the input-output map from v to e can be expressed as the following linear fractional transformation

$$e = F_u(G, \Delta)v$$

$$\text{where} \quad F_u(G, \Delta) = G_{22} + G_{21}\Delta(I - G_{11}\Delta)^{-1}G_{12} \ .$$

The nominal performance objective is simply

$$\| G_{22} \|_\infty = \sup_\omega \ \bar{\sigma}\left(G_{22}(jw)\right) \ .$$

Robust stability for unstructured uncertainty (only $\bar{\sigma}(\Delta) \leq 1$ known) depends on $\| G_{11} \|_\infty$. Unfortunately, norm bounds are inadequate for dealing with robust performance and realistic models of structured plant uncertainty. To handle these questions, the structured singular value, μ is used. μ is used to analyze linear fractional transformations when Δ has structure. A more complete background on μ can be found in [4-7].

3.2 Synthesis Review - H_∞ Optimization

For the purpose of synthesis, the Δ can be normalized via a transformation, and the transformation absorbed into P. This results in the synthesis problem in figure 4-(c). Hence, the synthesis problem involves finding a stabilizing controller K such that the performance requirements are satisfied with the inclusion of uncertainties. The interconnection structure P can be partitioned so that the input-output map from v' to e' can also be expressed as the following linear fractional transformation

$$e' = F_l(P, K)v'$$

where

$$F_l(P, K) = P_{11} + P_{12}K(I - P_{22}K)^{-1}P_{21} \ .$$

For H_∞ optimal control problem, the objective is to find a stabilizing controller K which minimizes $\| F_l(P, K) \|_\infty$.

A detailed review of H_∞ is given in [8] and state-space results are discussed in [5,6,9].

3.3 μ-Synthesis Methodology

The μ-synthesis methodology emerges as a practical approach in designing control systems with robust performance. This technique essentially integrates two powerful theories for synthesis and analysis into a systematic design technique that involves using the H_∞ optimization method for synthesis and the structured singular value (μ) for analysis. Since μ may be obtained by scaling and applying the $\| \cdot \|_\infty$, it can be reformulated as an H_∞ control design problem. The problem of robust controller design becomes one that find a stabilizing controller K and scaling matrix D such that the quantity

$$\| DF_l(P, K)D^{-1} \|_\infty$$

is minimized. One approach to solve this problem is to alternately minimizing the above expression for either K or D while holding the other constant.

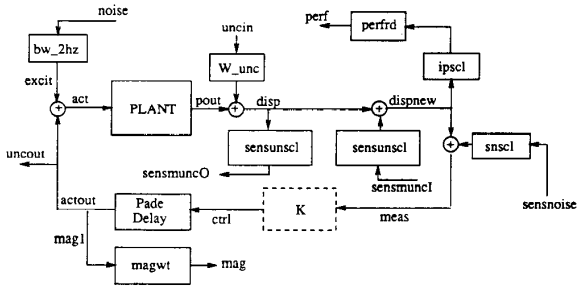

Figure 5: Problem Formulation

For fixed D, it becomes an H_∞ optimal control problem and can be solved using the well-known state-space method [5,6]. On the other hand, with fixed K, the problem can be minimized at each frequency as a convex optimization in $ln(D)$. The resulting data of D can be fit with an invertible, stable, minimum-phase, real-rational transfer function. This process is carried out iteratively until a satisfactory controller is constructed. Although, this iterative scheme does not guarantee to find a global optimum of the above minimization problem, in spite of this, the approach appears promising and consistent results have been obtained.

4 Control Problem Formulation

The μ-framework requires the designer to formulate the control problem in a linear fractional description. Figure 5 shows the block diagram of the problem formulation used in designing controller K_8 which was implemented on the JPL/AFAL Flexible Structure Testbed. The problem formulation requires to scaling of all the output errors to 1, so that when μ is less than 1, "robust performance" is achieved for the plant and uncertainty description defined by the interconnection structure P.

4.1 Single-Input/Single-Output Control Design

Initially, control laws are formulated for vibration attenuation of the first two boom-dish modes using only the hub actuators and sensors. The actuators and sensors are paired to regard the system as two decoupled SISO systems. The discrepancies between the real structure and the model are taken into account with uncertainty models. In the μ-framework, the characteristics of the system and associated uncertainties are included in the problem formulation.

There are several types of uncertainty which are prevalent in the design of control systems for this antenna experiment. These include: unmodeled dynamics, the level of damping in each flexible mode, and the gain levels of the actuators and sensors. The damping uncertainties and actuator magnitude levels are limiting factors in achieving a high performance vibration attenuation control design. The first set of control designs incorporated multiplicative sensor uncertainty to account for the damping uncertainty, gain variations in the actuators and sensors, and crosscoupling between the two single input/single output systems. An additive uncertainty is used to account for the neglected high frequency modes.

Mode Number	Frequency (Hertz)	Wave Number(k)
1	0.210	0
2	0.253 *	2
3	0.290 *	3
4	0.322 *	4
5	0.344 *	5
6	0.351	6
7	1.517	0
8	1.533 *	2
9	1.550 *	3
10	1.566 *	4
11	1.578 *	5
12	1.583	6
* two-fold degenerate modes		

Table 1. Modal Frequencies of Dish Modes

Mode Number	Frequency (Hertz)		Wave Number(k)
	1-7 Axis	4-10 Axis	
1	0.091	0.091	1
2	0.628	0.616	1
3	1.687	1.685	1
4	2.682	2.577	1
5	4.897	4.858	1
6	9.892	9.822	1

Table 2. Modal Frequencies of Boom-Dish Modes

In figure 5 the **PLANT** is a 2-input/2-output identified model consisting 2 decoupled two-mode SISO subsystems as reported in [1]. The two SISO transfer functions are:

$$\frac{HS1}{HA10} = \frac{3.2}{s^2+0.1654s+0.3753} + \frac{29.5}{s^2+0.1995s+15.9187}$$

and

$$\frac{HS10}{HA1} = \frac{5.2}{s^2+0.1313s+0.3563} + \frac{39}{s^2+0.0696s+14.9317}.$$

The additive uncertainty, W_{unc}, has a weighting function of $3.5\frac{s+1}{s+50}$. Output uncertainty associated with the sensors is formulated as multiplicative uncertainty on the sensor outputs and treated as a constant 16% uncertainty across the entire frequency range.

There is a constraint on the actuator torque which is incorporated as a performance constraint. The actuator signals are output as an error, **mag**, and weighted accordingly. The scalar weight, **magwt**, scales the actuator magnitude limit. In the controller design for K_8, the magnitude was limited to 1.11 Nm. In the experiment facility, the actual limitation on the actuator force is ± 2.3 Nm. The discrepancy is due to the model having too high of a damping value for the second mode, which leads to a difference of approximately a factor of 2 between theoretical and experimental actuator force levels. Sensor noise, on the order of ± 1 $mrad$, is taken into account in the problem formulation. A first order Pade approximation of the sample time is included, to account for the continuous time system being implemented in discrete time.

Finally, the performance specification on the closed-loop transfer function between input disturbance and output sensors is defined. The performance weight consists of a constant weighting of 2.2. This requires the peak value of the magnitude in the closed-loop transfer function between the disturbance and sensors be reduced by 2.2. Figure 5 can be easily rearranged into the control design interconnection structure shown in figure 6. One will notice that there is a significant amount of structure associated with the uncertainty descriptions and performance requirements. A straight H_∞ control design would not be able to take advantage of the knowledge of this structure, whereas controllers formulated using μ-synthesis can take advantage of this information.

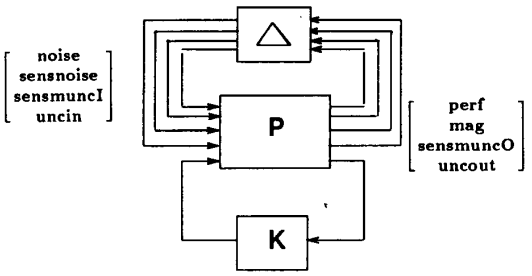

Figure 6: Control Design Interconnection Structure

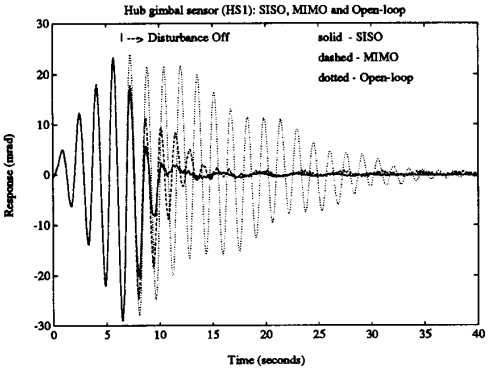

Figure 7: Response of Hub Gimbal Sensor HS1

4.2 Analysis and Experimental Results

Using the μ-synthesis techniques discussed earlier, a controller is designed for the interconnection structure shown in figure 6 . The controller size was on the order of 11 states for each input/output channel (2 channels). Due to limitations associated with implementing these control laws, the controller design was reduced in size using balanced minimal realization methods. The size of the controller implemented on the experiment is 5 states for each channel. There is a very small difference between the original control design Bode plots and the reduced order one. In the theoretical formulation, reduction in controller size showed little degradation in performance and robust tests. The prewarped Tustin method is used to discretize the analog control design. The sample rate is 20 Hz and 10 rad/s is used for the warping frequency.

The results of implementing controller K_8, is shown in figures 7 and 8. For the defined model set, (i.e. the nominal plant model with the uncertainties), the control law exhibited robust performance. Figure 7 shows the open-loop response of the structure, at hub gimbal sensor HS1, to 8 pulses of .8 second with $\pm$ 1 Nm torque level, the system is then allowed to decay to an ambient state. Figure 8 shows the response at the rib root sensor, RS4. The decay time is measured when the sensors are within 2 $mrad$ of a normal zero value. One will note that hub gimbal actuator HA10 is associated with the hub gimbal sensor HS1 with the torque measured in Nm and the output measured in $mrad$. This excitation pattern excites the second boom-dish mode of the structure. In the closed-loop experiment, the controller is switched on after the last pulse (6.4 seconds). A plot of the control action is shown in figure 9 for the hub gimbal actuator, HA10.

In a comparison of the open-loop response with the closed loop response, one can see that the decay time is significantly reduced. The difference in decay time between the closed loop and open loop system is on the order of a factor of 6. The controller uses a maximum of 2.3 Nm for actuator HA1 and 1.8 Nm for HA10.

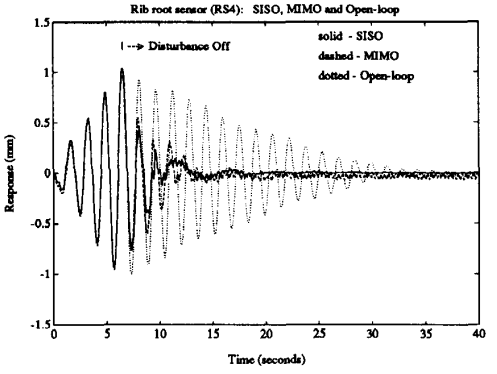

Figure 8: Response of Rib Root Sensor RS4

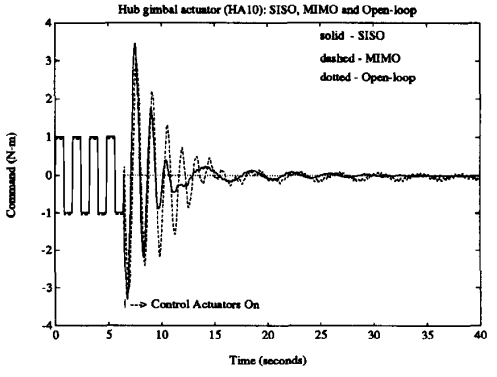

Figure 9: Control Action at HA10

4.3 Multivariable Control Designs

Several multivariable control laws were formulated for the JPL/AFAL antenna using a hub actuator/sensor pair and two collocated rib actuator/sensor pairs (i.e HA10/HS1, RA4/RS4 and RA10/RS10). The finite element model was used in control design. Due to the computational restrictions, only actuator/sensor pairs along 4-10 axis are used. The fact that the 1-7 axis and 4-10 axis are highly symmetric in the model, leads to little cross-coupling elements between the axes in the model. Therefore, the 1-7 and 4-10 axis control laws are designed independently.

For the multivariable designs, similar uncertainties are present as in the single-input/single-output control designs. Additional modes associated with the first rib bending mode are included in the design model along with the first two boom-dish modes. The neglected modes are taken into account by bounding their magnitude with a frequency domain additive uncertainty weight. A block diagram similar to figure 5 is used for control design with input multiplicative actuator uncertainty included along with output multiplicative sensor uncertainty.

The control design model developed using the finite element method varies from the experimental transfer functions. Specifically, there are noticeable differences between the identified transfer function for HA10/HS1 and the finite element model. Due to these discrepancies and others which might be present, a high level of uncertainty is used in the multivariable control formulation. Control K_{23} was designed with a additive uncertainty weight of $.8\frac{s+6}{s+60}$, and the input (49%) and output (1%) uncertainty levels are treated as a constant uncertainty across frequency. One would expect that a control design based on the identified model would have better performance than the one based on a finite element model.

4.4 Results

Figures 7 and 8 are plots of implementing the MIMO control law on the JPL/AFAL structure as compared with the SISO control law and open-loop. The decay time of the controller is 11 seconds for the same input excitation used in the open-loop and SISO cases. In spite of the fact that the multivariable control law used the additional actuators RA4 and RA10 and sensors RS4 and RS10, it performed worse that the SISO control law. It's performance is half that of the SISO design. This is attributed to the inaccuracies associated with the finite element models and the high level of uncertainty required to generate a robust multivariable design. It appears that K_{23} has too much gain at high frequency since it appears to be tracking some input noise. In future designs, the size of the additive uncertainty weight will be increased to alleviate this problem. The inclusion of a significant amount of uncertainty in the control design model was necessary to assure stability of the MIMO control laws when implemented on the real structure.

5 Conclusion

Using the μ-framework, we were able to synthesize control designs which performed well on the experimental system. To date, the SISO control law achieves the highest vibration attenuation of the antenna structure for the disturbances described. In the SISO design, the performance of the antenna experiment is limited by the actuator torque available. Increased actuator torque would certainly increase the performance capability of the structure.

The use of additional actuators/sensors should improve the performance characteristics of the closed-loop system. The reason this wasn't observed in the multivariable control designs is due to the use of an inaccurate model (i.e finite element model), in the control design. To improve performance of the MIMO control laws, more accurate models of the multivariable system are necessary.

Future work involving the JPL/AFAL flexible antenna experiment involves redesigning the multivariable control laws based on an improved model, when one becomes available. This work would include increasing the number of actuators/sensors used, and addressing the issue of non-collocated sensors and actuators. Additional sensors and actuators would allow more modes of the system to be damped and potentially increased vibration attenuation across the frequency spectrum of the structure. Robustness issues will also be addressed. The control designs will be tested to determine their robustness to different types of uncertainties associated with the plant, actuators, and sensors. Research in this same area is also being carried out at the California Institute of Technology [10,11].

Acknowledgement

The authors would like to thank Dr. S.J. Wang for his support for use of the experimental facility. Thanks are also due Dr. John Wen for providing the identification model and to Mr. Asif Ahmed for assisting in conducting the experiment. The research described in this paper was supported by Caltech President's Fund.

References

[1] H.C. Vivian, P.E. Blaire, D.B. Eldred, G.E. Fleischer, C.-H.C. Ih, N.M. Nerheim, R.E. Scheid, and J.T. Wen, "Flexible Structure Control Laboratory Development and Technology Demonstration," Final Report, JPL Publication 88-29, October 1, 1987.

[2] D.S Bayard, F.Y. Hadaegh, Y. Yam, R.E. Scheid, E. Metten and M.H Melnay, "Frequency Domain Identification Experiment on a Large Flexible Structure," American Control Conference (ACC), Pittsburgh, PA, June, 1989.

[3] J.C. Doyle, "Analysis of Feedback Systems with Structured Uncertainties," Proc. IEE-D 129, 1982, pp. 242-250.

[4] J.C. Doyle, "Lecture Notes on Advances in Multivariable Control," ONR/Honeywell Workshop on Advances in Multivariable Control, Minneapolis, MN, October, 1984.

[5] J.C .Doyle and C.C. Chu, "Robust Control of Multivariable and Large Scale Systems," Final Technical Report for AFOSR, Contract No. F49620-84-C-0088, March 1986.

[6] A.K. Packard, "What's New with μ: Structured Uncertainty in Multivariable Control," Ph.D. Thesis, University of California at Berkeley, 1988.

[7] B.A. Francis, *A Course in H_∞ Control Theory*, Springer-Verlag, Berlin, 1987.

[8] J.C. Doyle, K. Glover, P. Khargonekar and B.A. Francis, "State-Space Solutions to Standard H_2 and H_∞ Control Problems," ACC, Atlanta, GA, June, 1988.

[9] J.C. Doyle and C.C. Chu, "Matrix Interpolation Theory and H_∞ Performance Bounds," Automatic Control Conference, Boston, MA, June 1985.

[10] G.J. Balas and J.C. Doyle, "On the Caltech Experimental Large Space Structure," ACC, Atlanta, GA, June, 1988.

[11] G.J. Balas and J.C. Doyle, "Robust Control of Flexible Modes in the Controller Crossover Region," ACC, Pittsburg, PA, June, 1989.